Laboratory Research

https://doi.org/10.3340/jkns.2025.0245

Nintedanib Attenuates Epidural Fibrosis After Laminectomy in Rats

Kadri Kulualp,[1] Meltem Kumaş Kulualp,[2] Ziya Yurtal,[3] Sefa Kizildağ,[4] Beste Balbal Kandemir[4]

Department of Surgery,[1] Faculty of Veterinary Medicine, Dokuz Eylul University, Izmir, Turkey

Department of Histology and Embryology,[2] Faculty of Veterinary Medicine, Dokuz Eylul University, Izmir, Turkey

Department of Surgery,[3] Faculty of Veterinary Medicine, Hatay Mustafa Kemal University, Hatay, Turkey

Department of Medical Biology,[4] Faculty of Medicine, Dokuz Eylul University, Izmir, Turkey

Accepted article

Running title: Nintedanib Attenuates Epidural Fibrosis

• Received : November 25, 2025 • Revised: January 5, 2026 • Accepted : January 12, 2026

Address for correspondence : **Kadri Kulualp**

Department of Surgery, Faculty of Veterinary Medicine, Dokuz Eylul University, Izmir, Turkey

Tel : +90 (530) 500 9728, Fax : +90 , E-mail : kadri.kulualp@deu.edu.tr, ORCID : https://orcid.org/0000-0002-5877-0054

This is an Open Access article distributed under the terms of the Creative Commons Attribution Non-Commercial License (http://creativecommons.org/licenses/by-nc/4.0) which permits unrestricted non-commercial use, distribution, and reproduction in any medium, provided the original work is properly cited.

Copyright © 2026 The Korean Neurosurgical Society

Abstract

Objective : Epidural fibrosis (EF) is a major contributor to postoperative morbidity following laminectomy. This study investigated the antifibrotic, anti-inflammatory, and anti-angiogenic effects of nintedanib (NIN), a multi-tyrosine kinase inhibitor, in a rat model of post-laminectomy EF.

Methods : Twenty-one male Wistar albino rats were assigned to three groups: Control, Laminectomy (LAM), and Laminectomy + Nintedanib (NIN). The laminectomy procedure was performed at the L3 level. NIN administration, following laminectomy, was administered orally at a dose of 50 mg/kg/day for 28 days. Histopathological evaluations included hematoxylin-eosin staining for dura mater thickness and fibroblast density, and Masson's trichrome staining for collagen deposition and adhesion grading. α-smooth muscle actin (α-SMA) expression was evaluated using immunohistochemistry and RT-qPCR. Gene expression of tumor necrosis factor-α (TNF-α), interleukin-1β (IL-1β), vascular endothelial growth factor (VEGF), platelet-derived growth factor receptor (PDGFR), and transforming growth factor-β1 (TGF-β1) was quantified to characterize inflammatory, angiogenic, and fibrogenic responses. Statistical comparisons were conducted using one-way ANOVA or Kruskal–Wallis tests with appropriate post hoc analyses.

Results : The LAM group exhibited marked post-laminectomy changes, including increased dura mater thickness (8.20 ± 0.23 μm vs. 3.93 ± 0.08 μm in controls, $p < 0.0001$), elevated fibroblast density ($p = 0.0006$), severe collagen deposition, and high-grade epidural adhesions (Grade 3, $p = 0.0006$). NIN treatment attenuated these alterations, reducing dura mater thickness (4.80 ± 0.20 μm, $p < 0.0001$ vs. LAM), fibroblast density ($p < 0.01$), and adhesion grade (Grade 1, $p = 0.0012$). α-SMA immunoreactivity was high in LAM (Grade 3, $p < 0.0001$), whereas NIN significantly suppressed myofibroblast activation (Grade 1, $p = 0.0012$). NIN also significantly downregulated inflammatory mediators TNF-α ($p < 0.001$) and IL-1β ($p < 0.001$), as well as angiogenic markers VEGF ($p < 0.001$) and PDGF ($p < 0.001$), and fibrogenic mediators TGF-β1 ($p < 0.001$) and α-SMA ($p < 0.01$). These findings indicate that NIN suppresses fibroblast activation, extracellular matrix accumulation, and myofibroblast differentiation, thereby limiting epidural adhesion and scar maturation.

Accepted article

Conclusion : Nintedanib effectively mitigated epidural fibrosis after laminectomy through combined antifibrotic, anti-inflammatory, and anti-angiogenic actions. By improving the dural structure and reducing key molecules that contribute to scar formation, NIN shows significant promise as a treatment to prevent postoperative epidural adhesions. Future studies with extended follow-up may help clarify its clinical relevance.

Key Words : Laminectomy · Epidural fibrosis · Rat model · Nintedanib · Treatment.

INTRODUCTION

Accepted article

Spinal stenosis, intervertebral disc herniation, and degenerative or neoplastic disorders can compress the spinal cord or nerve roots, causing pain, paresis, or sensory deficits that impair quality of life [1,8]. Laminectomy, a common decompressive procedure, effectively relieves neural compression but often results in postoperative epidural fibrosis (EF) [8]. EF is initiated by local tissue disruption and hemorrhage, which triggers a robust inflammatory cascade and recruitment of neutrophils, macrophages, and lymphocytes [12]. These immune cells release proinflammatory cytokines (IL-1β, TNF-α), angiogenic mediators (VEGF, PDGF, FGF), and profibrotic factors (TGF-β), promoting fibroblast proliferation and their differentiation into myofibroblasts [6,12]. Progressive extracellular matrix (ECM) accumulation subsequently replaces normal epidural tissue with dense fibrotic adhesions, leading to recurrent pain, restricted neural mobility, and neurological impairment [6,12,29].

EF is a leading contributor to failed back surgery syndrome, reported in 8-40% of patients, with nearly one-fourth of cases directly related to fibrosis [8]. Because reoperation carries substantial risks, including dural tears and nerve root injury [20], pharmacological prevention is preferred over surgical reintervention [6,10,12].

The development of EF is driven by tightly interconnected inflammatory, angiogenic, and fibrogenic mechanisms [6,12]. Although numerous pharmacological agents and barrier materials have been evaluated, none have demonstrated reproducible or clinically meaningful efficacy [1,8,10,29].

Nintedanib (NIN), a multi-targeted tyrosine kinase inhibitor that blocks PDGFR, FGFR, and VEGFR, exhibits antifibrotic, anti-angiogenic, and anti-inflammatory activity [11,15]. NIN, an approved treatment for idiopathic pulmonary fibrosis [11], targets key mediators of fibrosis and angiogenesis; however, its potential therapeutic efficacy in post-laminectomy EF has not been investigated. Therefore, this study examined whether NIN attenuates laminectomy-induced EF by modulating the fibroinflammatory and angiogenic responses that underlie postoperative scar formation.

Accepted article

MATERIALS AND METHODS

Ethics statement

All experimental procedures were approved by the XXX University Animal Care and Ethics Committee (Approval No: 02/15/2023) and conducted in accordance with the NIH Guide for the Care and Use of Laboratory Animals and the ARRIVE guidelines.

Experimental design and surgical procedure

Twenty-one adult male Wistar albino rats (250-300 g) were housed in the Multidisciplinary Laboratory Animal Research Center of XXX University under controlled temperature (24 ± 1 °C), humidity (60 ± 10%), and a 12-hour light/dark cycle, with ad libitum access to food and water. All experimental procedures and surgical interventions were conducted in the same facility. Rats were randomly divided into three groups (n

= 7 each): Control, Laminectomy (LAM), and Laminectomy + Nintedanib (LAM+NIN). The control group received no intervention. The LAM group underwent an L3-level laminectomy [29], whereas the LAM+NIN group received oral nintedanib (50 mg/kg/day) for 28 days following surgery [2]. The NIN dosage was determined based on established experimental protocols in rodents, where NIN has demonstrated potent antifibrotic efficacy within a range of 30-100 mg/kg in mice and 10-50 mg/kg in rats [2, 24]. Specifically, a dose of 50 mg/kg has been successfully utilized in various organ fibrosis models to inhibit fibroinflammatory signaling without significant systemic toxicity [4, 14]. Regarding the duration, the 28-day administration period was selected to align with the established temporal progression of EF in rat models, ensuring that the pharmacological intervention covers the entire process from early inflammatory response to mature scar tissue formation and stabilization [10, 22, 29]. The assessment was conducted on postoperative day 28 as this single endpoint represents the phase of established, mature scar formation in rat laminectomy models [10, 29]. This timeline is widely accepted in experimental EF research to evaluate the definitive efficacy of pharmacological interventions on stabilized fibrotic tissue, rather than transient inflammatory phases [22, 29].

Anesthesia was induced with intraperitoneal ketamine (50 mg/kg) and xylazine (10 mg/kg). The lumbar region was shaved and disinfected with povidone-iodine, and a midline incision was made between L1 and L5. After paravertebral muscle dissection, a total L3 laminectomy was performed under aseptic conditions while preserving dural integrity. All surgical procedures were performed by the same surgical team using an operating microscope to ensure technical consistency and minimize inter-operator variability. Following microsurgical decompression and confirmation of dural integrity, hemostasis was achieved, and the wound was closed in layers with 4-0 polypropylene sutures. On postoperative day 28, all animals were euthanized under deep anesthesia, and spinal tissues were collected for analysis. To preserve the anatomical relationship between the laminectomy site, the dura mater, and the surrounding fibrotic tissue, the lumbar spinal specimens were harvested en bloc. Specifically, the L2-L4 vertebral segment, including the laminectomy area and associated paraspinal structures, was excised as a single unit using a high-speed surgical drill and

Accepted article

micro-rongeurs. This harvesting technique ensured that the epidural interface remained undisturbed for subsequent analysis.

A total of 21 rats completed the experimental protocol, and no perioperative or postoperative mortality occurred in any of the experimental groups throughout the study. To maximize the data yield from each experimental cohort and ensure a direct correlation between structural and molecular findings, an integrated experimental design was adopted [1, 3, 29]. Following euthanasia, the spinal tissue block from each animal (n=7 per group) was divided longitudinally into two symmetrical halves. One half was immediately fixed in 4% paraformaldehyde for histopathological and immunohistochemical evaluations, while the contralateral half was preserved in RNAlater solution and stored at -80°C for RT-qPCR assays. This methodology ensures that both histological and molecular analyses are derived from the same experimental subjects, enhancing methodological consistency and statistical reliability [10, 29].

Accepted article

Histopathological evaluation

Lumbar spinal specimens were fixed in 4% paraformaldehyde (pH 7.4) for 48 hours, decalcified in 10% ethylenediaminetetraacetic acid (EDTA) for four weeks with solution changes every three days, and embedded in paraffin. Serial 5-μm sections were mounted on poly-L-lysine-coated slides. Hematoxylin-eosin (H&E) staining was used to evaluate general morphology, while Masson's trichrome staining assessed collagen deposition and connective tissue organization. Histological examinations were performed using a Carl Zeiss Axiolab 5 microscope, and representative images were digitally recorded for morphometric analysis.

Epidural fibrosis was graded based on adhesion between the dura mater and surrounding tissues [20]: Grade 0, no fibrosis; Grade 1, thin fibrous bands limited to the dura; Grade 2, adhesions occupying up to two-thirds of the laminectomy defect; and Grade 3, extensive fibrosis exceeding two-thirds of the defect or extending to nerve roots. Dura mater thickness was measured at 400× magnification.

Fibroblast density was assessed by counting cells in three randomly selected regions (one central, two peripheral) at 400× magnification and graded as follows: Grade 1, <100 fibroblasts; Grade 2, 100-150; Grade 3, >150. All evaluations were performed by a blinded histologist to ensure objectivity and impartiality.

Immunohistochemistry

Paraffin-embedded 5-μm spinal sections were deparaffinized, rehydrated, and subjected to Tris-EDTA antigen retrieval (pH 9.0) at 95 °C. Endogenous peroxidase activity was quenched with 3% hydrogen peroxide, followed by blocking with 1% bovine serum albumin. Sections were incubated overnight at 4 °C with a mouse monoclonal anti-α-smooth muscle actin (α-SMA) antibody, followed by an HRP-conjugated secondary antibody. Immunoreactivity was visualized using DAB, and nuclei were counterstained with Mayer's hematoxylin. α-SMA staining intensity and distribution were evaluated semi-quantitatively by a blinded histologist using a four-point scale: Grade 0, no staining; Grade 1, <25% of cells; Grade 2, 25–50%; Grade 3, >50% (15). Scoring was performed based on the evaluation of multiple sections and multiple high-power fields per specimen, with a focus on fibroblast-rich areas within the epidural fibrosis region. This scoring system enabled comparative assessment of myofibroblast activation among the control, LAM, and LAM+NIN groups.

Accepted article

Molecular analyses

Tissue samples from the laminectomy area were preserved in RNAlater solution at 4°C overnight and stored at -80°C until analysis. Total RNA was extracted using TRIzol reagent, and purity and concentration were determined spectrophotometrically. Complementary DNA (cDNA) was synthesized from total RNA using a commercial reverse transcription kit according to the manufacturer's protocol.

Quantitative real-time PCR (RT-qPCR) was performed with the LightCycler 480 system using SYBR Green Supermix to measure mRNA expression of α-SMA, TGF-β1, VEGF, PDGF, TNF-α, and IL-1β. Primer sequences are presented in Table 1. GAPDH served as the reference gene. Cycling conditions were 95 °C for 30 seconds, followed by 40 cycles of 95 °C for 15 seconds and 60 °C for 1 minute. Relative gene expression levels were calculated using the 2^-ΔΔCt method. All reactions were performed in duplicate, and results were expressed as fold changes relative to the control group.

Statistical analysis

All statistical analyses were performed using GraphPad Prism version 9.0 (GraphPad Software, San Diego, CA, USA). Data were expressed as mean ± standard error of the mean (SEM) for continuous variables and as median (minimum-maximum) for ordinal data. The Shapiro-Wilk test was used to assess the normality of the data. Normally distributed data were analyzed using one-way ANOVA followed by Tukey's post hoc test; nonparametric data were evaluated with the Kruskal-Wallis test, and pairwise comparisons were performed with the Mann-Whitney U test. A p-value < 0.05 was considered statistically significant.

Accepted article

RESULTS

Histopathological evaluation

Hematoxylin-eosin (H&E) staining revealed distinct differences in dural architecture and peridural tissue among the groups. In the control group, the dura mater was thin, uniform, and clearly demarcated from adjacent tissues (Figure 1a), exhibiting a mean thickness of 3.93 ± 0.08 μm. In contrast, the LAM group showed pronounced disruption of dural structure, characterized by irregular thickening, fibrotic extension into the dural margins, and dense cellular infiltration (Figure 1b). The mean dura mater thickness in this

group increased to 8.20 ± 0.23 μm ($p < 0.0001$ vs. control; Figure 1d). In the LAM+NIN group, dural morphology was largely preserved, and peridural fibrotic expansion was visibly reduced compared with LAM (Figure 1c). The mean dural thickness was 4.80 ± 0.20 μm, significantly lower than that of the LAM group ($p < 0.0001$; Figure 1d).

Fibroblast density was minimal in the control group and markedly elevated in LAM, with widespread cellular proliferation and expansion of fibrotic areas ($p = 0.0006$; Figure 1e). Treatment with NIN significantly decreased fibroblast density compared with LAM ($p = 0.0035$), limiting fibroblast accumulation primarily to the peridural region (Figures 1c, e).

Accepted article

Epidural fibrosis and adhesion grading

Masson's trichrome staining demonstrated preserved epidural space and minimal collagen deposition in the control group (Grade 0; Figure 2a). In the LAM group, extensive EF was observed, characterized by dense collagen bundles, thick fibrotic bands, and firm adhesions between the dura mater and paravertebral tissues (Grade 3; $p = 0.0006$ vs. control; Figures 2b, d). In the LAM+NIN group, fibrotic tissue deposition and adhesion severity were markedly reduced, and the epidural space was largely maintained. The fibrosis grade was significantly lower compared with the LAM group (Grade 1; $p = 0.0012$; Figures 2c, d).

Immunohistochemistry (α-SMA)

α-smooth muscle actin (α-SMA) immunostaining demonstrated no fibroblastic α-SMA positivity in the dura or epidural space of the control group, where staining was restricted to vascular smooth muscle cells (Figure 3a). The LAM group exhibited diffuse α-SMA-positive fibroblasts in the epidural area (Figure 3b), with a median immunoreactivity score of Grade 3 ($p < 0.0001$ vs. control; Figure 3d). In the LAM+NIN group, α-SMA immunoreactivity was markedly reduced, presenting a more focal staining pattern (Figure 3c).

Accordingly, the median α-SMA score in this group was Grade 1, which was significantly lower than in the LAM group ($p = 0.0012$; Figure 3d). Although it remained slightly higher than in the controls ($p = 0.03$), it was still significantly lower than in the LAM group.

Gene expression analysis (RT-qPCR)

RT-qPCR revealed that expression levels of TNF-α and IL-1β were significantly elevated in the LAM group compared with controls (both $p < 0.0001$; Figures 4a, b). NIN treatment significantly downregulated both cytokines, reducing their expression to near-control levels ($p < 0.0001$ vs. LAM; Figures 4a, b).

The angiogenesis-related genes VEGF and PDGFR were similarly upregulated in LAM ($p < 0.0001$; Figures 5a, b), consistent with postoperative vascular proliferative activity. NIN markedly reduced the expression of both genes ($p < 0.0001$ vs. LAM; Figures 5a, b).

Fibrogenic markers also showed significant postoperative induction. TGF-β1 expression increased markedly in the LAM group ($p < 0.0001$; Figure 6a), whereas NIN significantly suppressed this elevation ($p < 0.0001$; Figure 6a). Expression of α-SMA mRNA was similarly elevated following laminectomy ($p < 0.0001$; Figure 6b) and significantly reduced by NIN administration ($p < 0.0001$; Figure 6b), consistent with immunohistochemical findings.

Accepted article

DISCUSSION

Epidural fibrosis (EF) is a major postoperative complication characterized by fibroblast proliferation, excessive ECM deposition, and adhesion formation around the dura mater [3,12]. This progressive fibrotic response may ultimately compress neural structures and contribute to failed back surgery syndrome [3].

Following surgical trauma and hemorrhage, the resulting inflammatory cascade promotes fibroblast recruitment and ECM overproduction [12]. Key mediators, including TGF-β, TNF-α, IL-1β, VEGF, and PDGF, act synergistically to drive myofibroblast differentiation and stimulate excessive collagen synthesis. Sustained activation of these signaling pathways reinforces ECM accumulation, enhances contractile phenotypic transitions, and perpetuates the cycle of pathological tissue remodeling [6,12].

Nintedanib (NIN), a multi-targeted tyrosine kinase inhibitor, exerts potent antifibrotic, anti-inflammatory, and anti-angiogenic effects through inhibition of PDGFR, FGFR, and VEGFR signaling pathways [18,28]. By blocking these upstream mediators, NIN suppresses fibroblast proliferation and migration, limits excessive ECM deposition, and inhibits the differentiation of fibroblasts into contractile myofibroblasts. Additionally, NIN downregulates key profibrotic molecules, including TGF-β and procollagen type I, which are central drivers of fibrotic remodeling [9]. Through this multimodal mechanism, NIN represents a strong therapeutic candidate capable of modulating the interdependent inflammatory, angiogenic, and fibrogenic processes underlying postoperative EF. Accordingly, this study investigated whether NIN could attenuate fibrosis and adhesion formation after laminectomy by targeting these convergent pathways.

Beyond its established antifibrotic properties, the biological effects of NIN can be mechanistically explained through its simultaneous inhibition of PDGFR, FGFR, and VEGFR, which converge on several downstream intracellular signaling cascades implicated in fibrotic remodeling. Experimental studies have demonstrated that blocking PDGFR and FGFR signaling suppresses fibroblast proliferation and migration, while inhibiting VEGFR interferes with angiogenesis-driven fibroblast activation and extracellular matrix accumulation [24, 27]. At the molecular level, NIN has been shown to attenuate TGF-β–dependent profibrotic signaling, including Smad-mediated transcriptional activity, thereby limiting myofibroblast differentiation and collagen synthesis [9, 28]. In parallel, inhibition of the MAPK/ERK and PI3K/Akt pathways has been reported to contribute to reduced fibroblast survival, acquisition of a contractile phenotype, and decreased extracellular matrix production in various fibrotic disease models [15, 17, 27]. Although these intracellular pathways were not directly interrogated in the present study, the observed

Accepted article

downregulation of TGF-β1 and α-SMA expression, together with reduced fibroblast density and epidural adhesion, is consistent with the established molecular actions of NIN reported in experimental fibrosis models [9, 15, 24, 28].

Histological analysis demonstrated pronounced post-laminectomy alterations in the LAM group, including marked dural thickening, substantial fibroblast proliferation, and extensive epidural adhesions, all characteristic indicators of active fibrotic remodeling. These findings align with previous reports that identify dural hypertrophy and fibroblast accumulation as central histopathological hallmarks in the progression of EF [5,22]. In contrast, NIN treatment markedly reduced these alterations, as reflected by a thinner dura mater, decreased fibroblast density, and substantially diminished epidural adhesions. These improvements suggest that NIN inhibits fibroblast activation and restricts ECM accumulation, thereby interrupting the fibrotic cascade. Similar antifibrotic effects have been demonstrated in pulmonary [27], hepatic [30], and renal [4] fibrosis models, where NIN attenuated collagen deposition and tissue stiffness by limiting fibroblast activity. Collectively, these observations show that NIN substantially reduces the histopathological severity of EF and provides a structural foundation for its downstream antifibrotic, anti-inflammatory, and anti-angiogenic molecular effects.

Inflammation represents the initiating and central phase of EF pathogenesis, with cytokines such as TNF-α and IL-1β promoting fibroblast proliferation and their transition into a profibrotic phenotype [6,12]. In this study, TNF-α and IL-1β expression levels were significantly increased in the LAM group, confirming postoperative inflammatory activation. NIN treatment markedly reduced both cytokines, consistent with its demonstrated anti-inflammatory effects in pulmonary [24], hepatic [26], and peritoneal [14] fibrosis models. These findings suggest that NIN suppresses early inflammatory signaling by downregulating TNF-α- and IL-1β-mediated pathways, thereby limiting fibroblast activation and reducing subsequent fibrotic remodeling.

Angiogenic signaling serves as a key intermediary in EF progression, linking postoperative inflammation to downstream fibrotic remodeling. Following surgical injury, VEGF and PDGF promote endothelial

Accepted article

proliferation and neovascularization, processes that facilitate ECM accumulation and expansion of fibrotic tissue [21]. Consistent with observations in pulmonary [16] and hepatic [13] fibrosis models, both angiogenic markers were significantly elevated in the LAM group, supporting their roles in fibroblast proliferation and scar maturation. NIN treatment significantly reduced VEGF and PDGF expression, in line with its inhibitory effects on PDGFR- and VEGFR-dependent pathways [18,28]. By suppressing these angiogenic and proliferative signals, NIN disrupts the pathological connection between vascular remodeling and fibrosis, contributing to reductions in fibroblast density, dural thickening, and epidural adhesion.

Fibrogenic signaling is a central driver of EF, primarily mediated by TGF-β1, which promotes fibroblast differentiation, ECM synthesis, and collagen deposition [3,21]. Sustained activation of the TGF-β1/Smad axis leads to excessive ECM accumulation and progressive scar maturation, reinforcing a self-perpetuating fibrotic loop. In the present study, TGF-β1 expression was significantly increased in the LAM group, underscoring its pivotal role in postoperative fibrogenesis. In contrast, NIN markedly reduced TGF-β1 levels, consistent with reports showing its capacity to inhibit TGF-β1-driven signaling and downregulate profibrotic mediators, such as collagen type I and fibronectin [7, 23]. This suppression indicates that NIN effectively targets the core fibrogenic pathway in EF, thereby disrupting the feedback mechanisms that sustain fibroblast activation and ECM deposition.

The fibroblast-to-myofibroblast transition is a pivotal event in fibrosis, with α-SMA serving as its principal marker [3,6,12,21]. In this study, α-SMA expression was markedly elevated in the LAM group, consistent with previous reports indicating that increased α-SMA reflects enhanced myofibroblast activity and ECM synthesis in fibrotic tissues [10,19]. NIN treatment significantly reduced α-SMA levels, as demonstrated by both immunohistochemistry and RT-qPCR, indicating effective suppression of myofibroblast differentiation. This finding is consistent with pulmonary [17], hepatic [25], and renal [4] fibrosis models, where NIN mitigated α-SMA upregulation and tissue remodeling. The concordance between molecular and histological outcomes further supports NIN's inhibitory effect on myofibroblast activation and persistence in fibrotic tissue.

Accepted article

Preventing postoperative EF remains a significant challenge, as traditional clinical strategies have primarily relied on passive physical barrier materials. These include absorbable hemostatic agents, such as Gelfoam, hyaluronate-based membranes, and various biologic or synthetic spacers, which aim to mechanically separate the dura mater from surrounding tissues during the early healing phase [1, 3, 22, 29]. While these approaches may reduce tissue adhesion by providing a physical shield, their efficacy remains variable because they do not directly modulate the underlying biological processes (such as inflammatory signaling and fibroblast activation) that drive fibrogenesis [6, 12]. In contrast, NIN offers a fundamentally different therapeutic strategy by actively targeting multiple upstream signaling pathways involved in fibroblast activation, angiogenesis, and inflammatory amplification. By inhibiting PDGFR, FGFR, and VEGFR signaling, NIN interferes with fibroblast proliferation, myofibroblast differentiation, and pathological neovascularization, thereby addressing the core molecular mechanisms responsible for epidural scar formation rather than merely acting as a physical shield [9, 11, 24, 27]. This multi-targeted biological activity represents a theoretical advantage over single-mechanism physical barriers, particularly in settings where inflammation-driven fibrosis predominates. Nevertheless, the absence of a direct head-to-head comparison between NIN and established clinical barrier materials constitutes an important limitation of the present study. Future investigations incorporating comparative experimental designs are warranted to determine whether pharmacological modulation of these fibroinflammatory pathways provides superior or additive protection against EF compared with conventional barrier-based strategies [6, 21].

Furthermore, the present evaluation was conducted exclusively on postoperative day 28, as this single endpoint corresponds to the peak histological and mechanical maturity of EF in rodent models [10, 22, 29]. While longitudinal assessments at earlier time points could provide insights into the early transition from acute inflammation to granulation tissue, the 28-day mark is widely accepted as a reliable and standard time point for evaluating the definitive efficacy of therapeutic interventions on established, mature scar tissue [10, 29]. This timeline ensures that the observed reduction in fibrosis reflects a sustained pharmacological

Accepted article

effect on stabilized fibrotic tissue rather than a temporary delay in the initial inflammatory response [22, 29].

Although oral administration of NIN at a dose of 50 mg/kg/day for 28 days was effective in attenuating EF in the present experimental model, the potential limitations of systemic delivery should be carefully considered in the context of clinical translation. Theoretically, NIN is associated with gastrointestinal disturbances, hepatotoxicity, and a potential risk for increased bleeding due to its potent inhibition of VEGF signaling [9, 24]. However, in our study, we did not observe any intraoperative or postoperative bleeding events, epidural hematoma formation, or wound-related complications in the treatment groups during the 28-day study period prior to euthanasia. This finding is consistent with previous experimental reports where similar doses and durations of NIN were utilized across different fibrosis models without resulting in significant systemic adverse effects [4, 11, 15, 24]. Nevertheless, while oral dosing was selected to establish proof-of-concept efficacy [18], the study was not specifically designed to quantitatively assess coagulation parameters. Therefore, long-term systemic administration in postoperative patients may carry clinical risks, and future investigations should focus on localized delivery strategies, such as drug-loaded hydrogels or biodegradable scaffolds, to achieve targeted antifibrotic effects at the surgical site while further minimizing systemic exposure and potential bleeding risks [3, 6, 22].

Accepted article

CONCLUSION

This study demonstrates that NIN effectively attenuates EF after laminectomy by targeting multiple interconnected pathogenic mechanisms. Histologically, NIN reduced dura mater thickening, fibroblast density, and epidural adhesion, while molecular analyses showed downregulation of key inflammatory (TNF-α and IL-1β), angiogenic (VEGF and PDGF), and fibrogenic (TGF-β1 and α-SMA) mediators.

Together, these findings indicate that NIN suppresses fibroblast activation, ECM deposition, and myofibroblast differentiation, which are central processes driving postoperative fibrotic remodeling.

AUTHORS' DECLARATION

Conflicts of interest

No potential conflict of interest relevant to this article was reported.

Accepted article

Informed consent

This type of study does not require informed consent.

Data sharing

None

Preprint

None

ORCID

Kadri Kulualp https://orcid.org/0000-0002-5877-0054

Meltem Kumaş Kulualp https://orcid.org/0000-0001-6903-3212

Ziya Yurtal https://orcid.org/0000-0001-6080-1860

Sefa Kizildağ https://orcid.org/0000-0001-7939-5153

Beste Balbal Kandemir https://orcid.org/0000-0003-1407-2497

References

Accepted article

1. Bahrami R, Akbari E, Rasras S, Jazayeri N, Khodayar MJ, Foruozandeh H, et al. Effect of local N-acetyl-cysteine in the prevention of epidural fibrosis in rat laminectomy model. **Asian J Neurosurg** 13(3): 664-668, 2018.

2. Bonella F, Stowasser S, Wollin L. Idiopathic pulmonary fibrosis: current treatment options and critical appraisal of nintedanib. **Drug Des Devel Ther** 9: 6407-6419, 2015.

3. Ding Q, Wei Q, Sheng G, Wang S, Jing S, Ma T, et al. The preventive effect of decorin on epidural fibrosis and epidural adhesions after laminectomy. **Front Pharmacol** 12: 774316, 2021.

4. Feng L, Li W, Chao Y, Huan Q, Lu F, Yi W, et al. Synergistic inhibition of renal fibrosis by nintedanib and gefitinib in a murine model of obstructive nephropathy. **Kidney Dis (Basel)** 7(1): 34-49, 2021.

5. Fouad S, Abass M, Rizk A, Mosbah E, Nabeeh MM, Elmezayyen AS, et al. The augmentative role of chitosan and platelet-rich fibrin in reducing epidural fibrosis after laminectomy in rats. **Eur J Med Res** 30(1): 749, 2025.

6. Ganesh V, Kancherla Y, Igram CM, Pugely AJ, Salem AK, Shin K, et al. Pharmacotherapies to prevent epidural fibrosis after laminectomy: a systematic review of in vitro and in vivo animal models. **Spine J** 23(10): 1471-1484, 2023.

7. Gunatilaka A, Zhang S, Tan WSD, Stewart AG. Anti-fibrotic strategies and pulmonary fibrosis. Adv **Pharmacol** 98: 179-224, 2023.

8. Ismailoglu O, Kizilay Z, Cetin NK, Topcu A, Berber O. Effect of curcumin on the formation of epidural fibrosis in an experimental laminectomy model in rats. **Turk Neurosurg** 29(3): 440-444, 2019.

9. Joannes A, Voisin T, Morzadec C, Letellier A, Gutierrez FL, Chiforeanu DC, et al. Anti-fibrotic effects of nintedanib on lung fibroblasts derived from patients with progressive fibrosing interstitial lung diseases. **Pulm Pharmacol Ther** 83: 102267, 2023.

10. Karagedik MI, Yuksel U, Kartal B, Ceylan AF, Ogden M, Bakar B. Evaluation of the effectiveness of oxytocin and enalapril in the prevention of epidural fibrosis developed after laminectomy in rats. **Injury** 54(7): 110793, 2023.

11. Lamb YN. Nintedanib: a review in fibrotic interstitial lung diseases. **Drugs** 81: 575-586, 2021.

12. Lewik G, Müller LS, von Glinski A, Schulte TL, Lange T. Postoperative epidural fibrosis: challenges and opportunities—a review. **Spine Surg Relat Res** 8(2): 133-142, 2024.

13. Li S, Guo X, Zhang T, Wang N, Li J, Xu P, et al. Fibroblast growth factor 21 ameliorates high glucose-induced fibrogenesis in mesangial cells through inhibiting STAT5 signaling pathway. **Biomed Pharmacother** 93: 695-704, 2017.

14. Liu F, Yu C, Qin H, Zhang S, Fang L, Wang Y, et al. Nintedanib attenuates peritoneal fibrosis by inhibiting mesothelial-to-mesenchymal transition, inflammation and angiogenesis. **J Cell Mol Med** 25(13): 6103-6114, 2021.

Accepted article

15. Pan L, Cheng Y, Yang W, Wu X, Zhu H, Hu M, et al. Nintedanib ameliorates bleomycin-induced pulmonary fibrosis, inflammation, apoptosis, and oxidative stress by modulating PI3K/Akt/mTOR pathway in mice. **Inflammation** 46: 1-12, 2023.

16. Qin X, Jia C, Liang J, Chen J, Liu X, Chao Z, et al. PEDF is an anti-fibrosis factor that inhibits fibroblast activation in a bleomycin-induced pulmonary fibrosis rat model. **Respir Res** 23: 100, 2022.

17. Roger I, Montero P, Milara J, Cortijo J. Pirfenidone and nintedanib attenuate pulmonary artery endothelial and smooth muscle cell transformations induced by IL-11. **Eur J Pharmacol** 972: 176547, 2024.

18. Srivali N, De Giacomi F. Benefit of antifibrotic therapy initiated during acute exacerbation of interstitial lung disease: a systematic review. **Respir Investig** 63(5): 755-761, 2025.

19. Saito S, Ohno SI, Harada Y, Kanno Y, Kuroda M. MiR-34a induces myofibroblast differentiation from renal fibroblasts. **Clin Exp Nephrol** 27(5): 411-418, 2023.

20. Tanriverdi O, Yilmaz I, Adilay HU, Gunaldi O, Erdogan U, Gungor A, et al. Effect of cetuximab on the development of epidural fibrosis based on CD105 and osteopontin immunohistochemical staining. **Spine (Phila Pa 1976)** 44(3): 134-143, 2019.

21. Tien CH, Wu YR, Cheng Y, Hsu YH. Targeting IL-20 alleviates inflammatory mechanical allodynia and reduces epidural fibrosis in a post-laminectomy syndrome rat model. Int Int **Immunopharmacol** 146: 113882, 2025.

22. Turkoglu E, Dinc C, Tuncer C, Oktay M, Serbes G, Sekerci Z. Use of decorin to prevent epidural fibrosis in a post-laminectomy rat model. **Eur J Pharmacol** 724: 86-91, 2014.

23. Wan Q, Li D, Shang S, Wu H, Chen F, Li Q. Novel synergistic therapeutic approach in idiopathic pulmonary fibrosis: combining nintedanib with baricitinib. **Pulm Pharmacol Ther** 89: 102346, 2025.

Accepted article

24. Wollin L, Maillet I, Quesniaux V, Holweg A, Ryffel B. Antifibrotic and anti-inflammatory activity of the tyrosine kinase inhibitor nintedanib in experimental models of lung fibrosis. **J Pharmacol Exp Ther** 349(2): 209-220, 2014.

25. Wu YT, Li QZ, Wu YQ, Mu M, Wu H, Tian HY, et al. Nintedanib attenuates NLRP3 inflammasome-driven liver fibrosis by targeting Src signaling. **Int Immunopharmacol** 143(Pt 3): 113630, 2024.

26. Yamanaka T, Harimoto N, Yokobori T, Muranushi R, Hoshino K, Hagiwara K, et al. Nintedanib inhibits intrahepatic cholangiocarcinoma aggressiveness via suppression of cytokines extracted from activated cancer-associated fibroblasts. **Br J Cancer** 122(7): 986-994, 2020.

27. Yang W, Pan L, Cheng Y, Wu X, Tang B, Zhu H, et al. Nintedanib alleviates pulmonary fibrosis in vitro and in vivo by inhibiting the FAK/ERK/S100A4 signaling pathway. **Int Immunopharmacol** 113(Pt A): 109409, 2022.

28. Yin Y, Liu S, Pu L, Luo J, Liu H, Wu W. Nintedanib prevents TGF-β2–induced epithelial-mesenchymal transition in retinal pigment epithelial cells. **Biomed Pharmacother** 161: 114543, 2023.

29. Yurtal Z, Kulualp K, Ozkan H, Micili SC, Dogan H, Sisman AR, et al. Protective and therapeutic effects of bovine amniotic fluids collected in different trimesters on epidural fibrosis after experimental laminectomy in rats. **World Neurosurg** 171: e722-e730, 2023.

30. Zeinali S, Bichsel CA, Hobi N, Funke M, Marti TM, Schmid RA, et al. Human microvasculature-on-a-chip: anti-neovasculogenic effect of nintedanib in vitro. **Angiogenesis** 21(4): 861-871, 2018.

Accepted article

Figure Legends

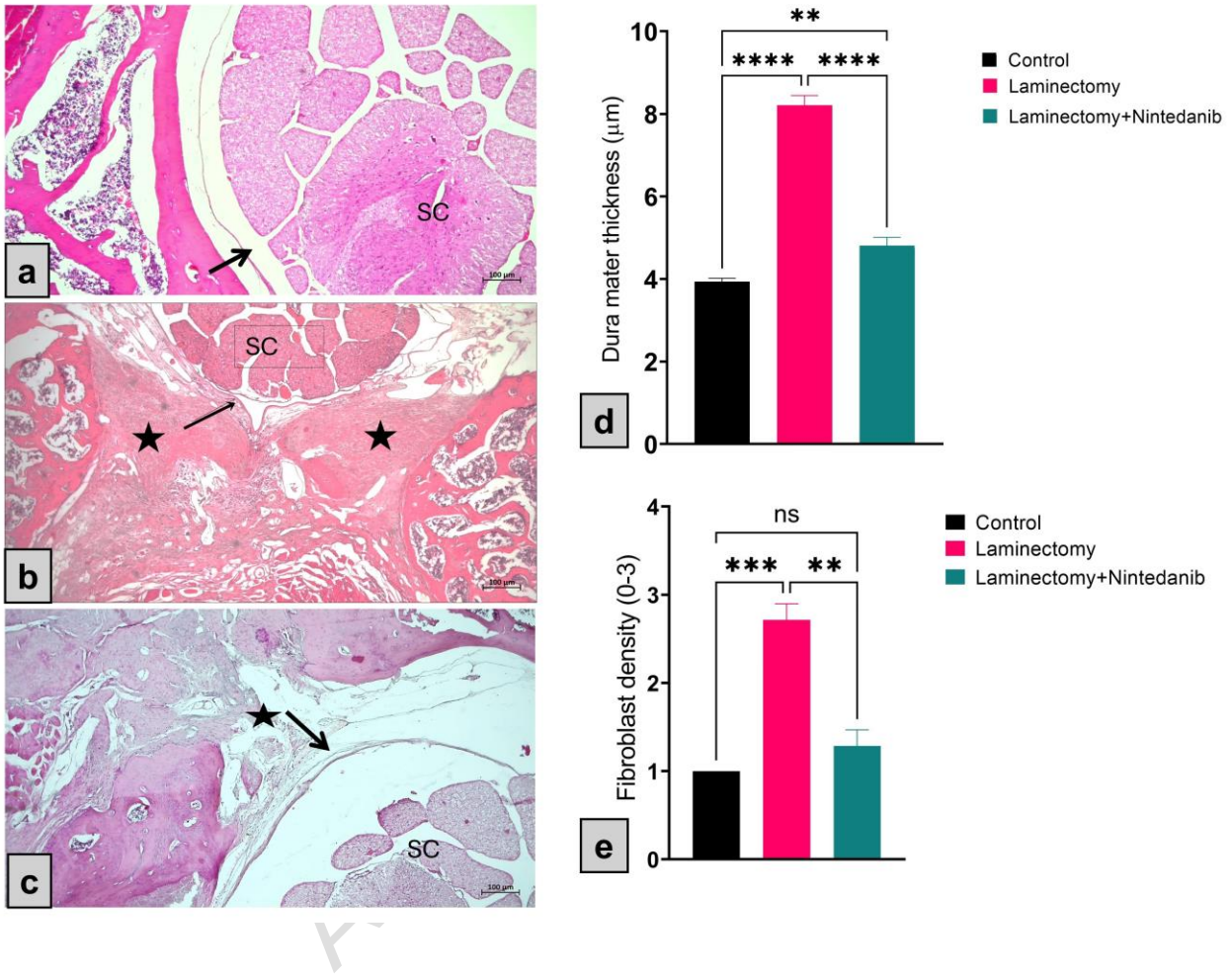


Fig. 1. Representative H&E staining and quantitative analyses of dura mater thickness and fibroblast density following laminectomy. (a) Control group: The dura mater appears thin, well-defined, and structurally homogeneous (arrow). Fibroblast density in the epidural space is minimal. (b) Laminectomy group: The dura mater is markedly thickened (arrow), with loss of normal boundaries and extensive fibroblast proliferation (★). (c) Laminectomy + Nintedanib group: The dura mater architecture is largely preserved, with reduced dural thickening and limited fibroblast accumulation (★). SC: spinal cord. All images were acquired at the same magnification (50×). Scale bar = 100 μm. (d) Quantitative comparison of dura mater thickness (μm). (e) Fibroblast density scores (0-3). Data are presented as mean ± SE, n=7. Statistical analysis:

One-way ANOVA with Tukey's post hoc test (**p < 0.01, ***p < 0.001, ****p < 0.0001; ns: not significant).

Accepted article

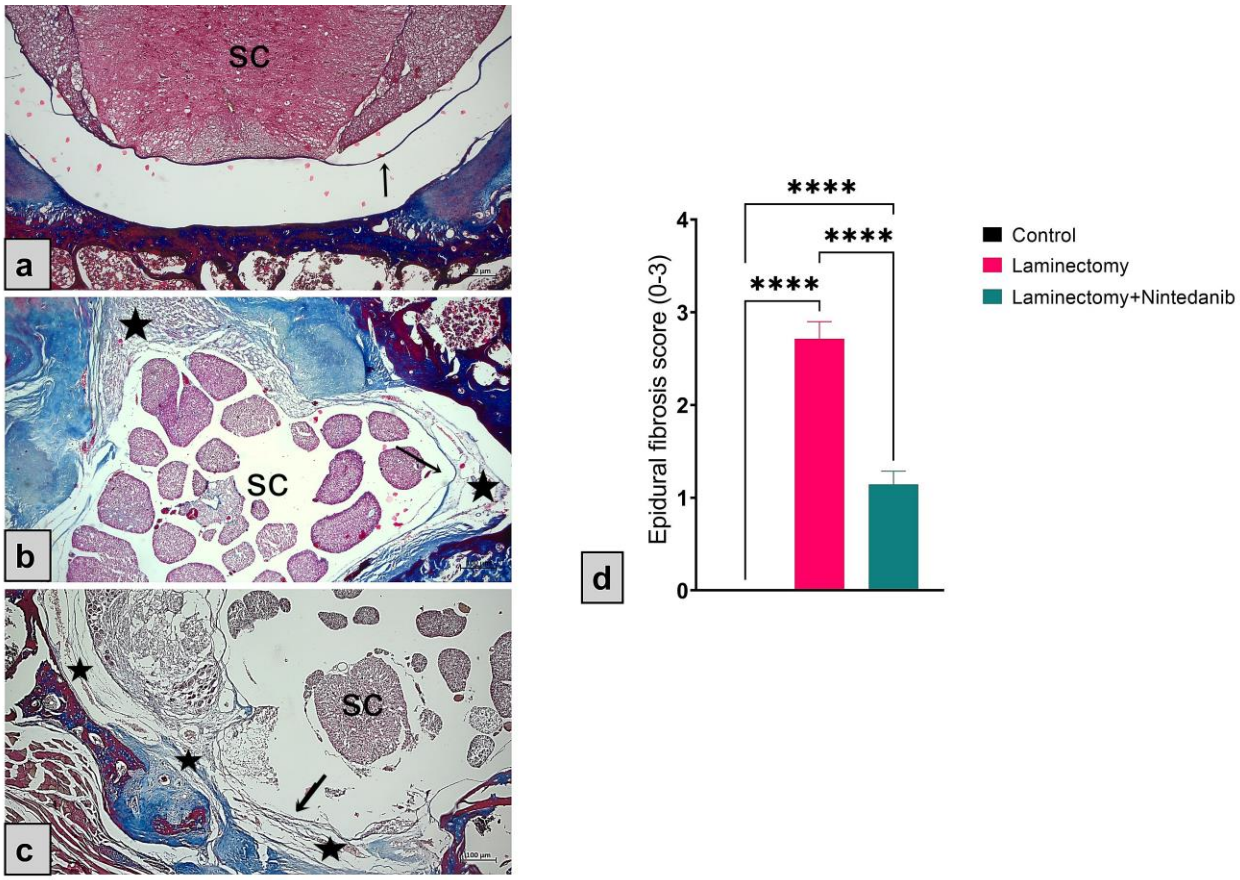


Fig. 2. Representative Masson's trichrome staining and evaluation of epidural fibrosis and dural adhesion. (a) Control group: The dura mater is well-defined (arrow), and the epidural space is clear with minimal collagen deposition. (b) Laminectomy group: Dense collagen accumulation (blue staining, ★) and fibrotic bands result in marked epidural adhesion. (c) Laminectomy + Nintedanib group: Collagen deposition is reduced and localized (★), with better preservation of the dura-epidural interface. SC: spinal cord. All images were acquired at the same magnification (50×, n = 7). Scale bar = 100 μm. (d) Epidural fibrosis scores (0-3). Data are presented as median (minimum-maximum). Statistical analysis: Kruskal-Wallis test with Mann-Whitney U test for pairwise comparisons (**$p < 0.01$, ***$p < 0.001$).

Accepte

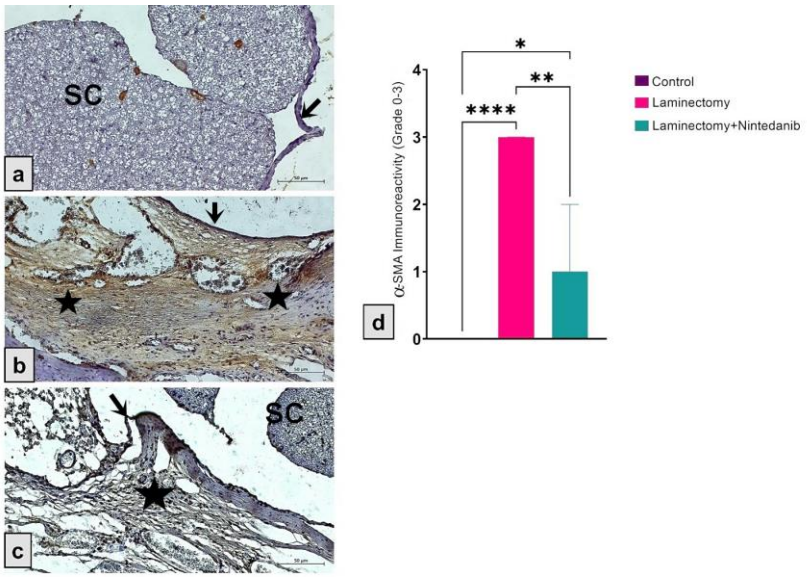


Fig. 3. Representative α-SMA immunohistochemistry in epidural tissues and immunoreactivity scores. (a) Control group showing well-defined dura mater (arrow) and minimal α-SMA expression. (b) Laminectomy group showing extensive α-SMA-positive myofibroblast accumulation within the epidural fibrotic tissue (★). (c) Laminectomy + Nintedanib group showing reduced and more focal α-SMA staining. α-SMA immunoreactivity scores were evaluated within the epidural fibrotic region using multiple high-power fields per specimen. Staining: α-SMA (HRP-DAB), hematoxylin counterstaining. SC: spinal cord. All images were acquired at the same magnification (100×); Scale bar = 50 μm. (d) Comparison of α-SMA immunoreactivity scores. Data are presented as median (minimum-maximum, n = 7). Statistical analysis: Kruskal-Wallis test with Mann–Whitney U test (*$p < 0.05$, **$p < 0.01$, ****$p < 0.0001$; ns: not significant).

Accepted article

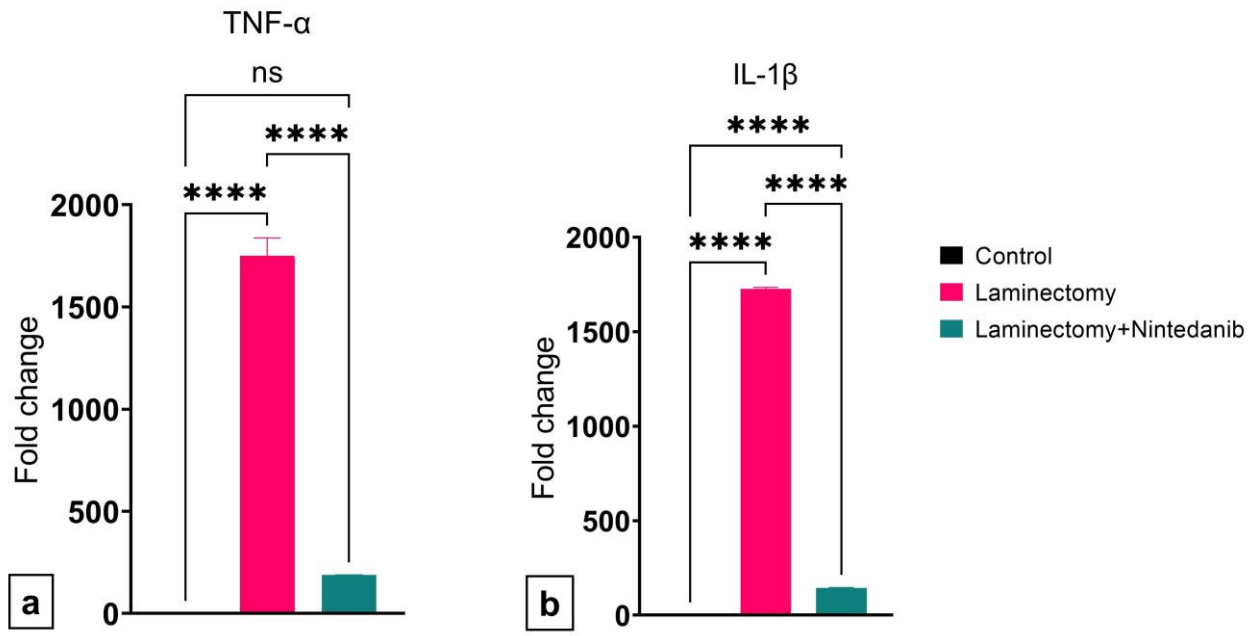


Fig. 4. Quantitative analysis of inflammatory markers by RT-qPCR. (a) TNF-α mRNA expression. (b) IL-1β mRNA expression. Data are presented as mean ± SE. Statistical analysis: One-way ANOVA with Tukey's post hoc test (****$p < 0.0001$; ns: not significant).

Accepted artic

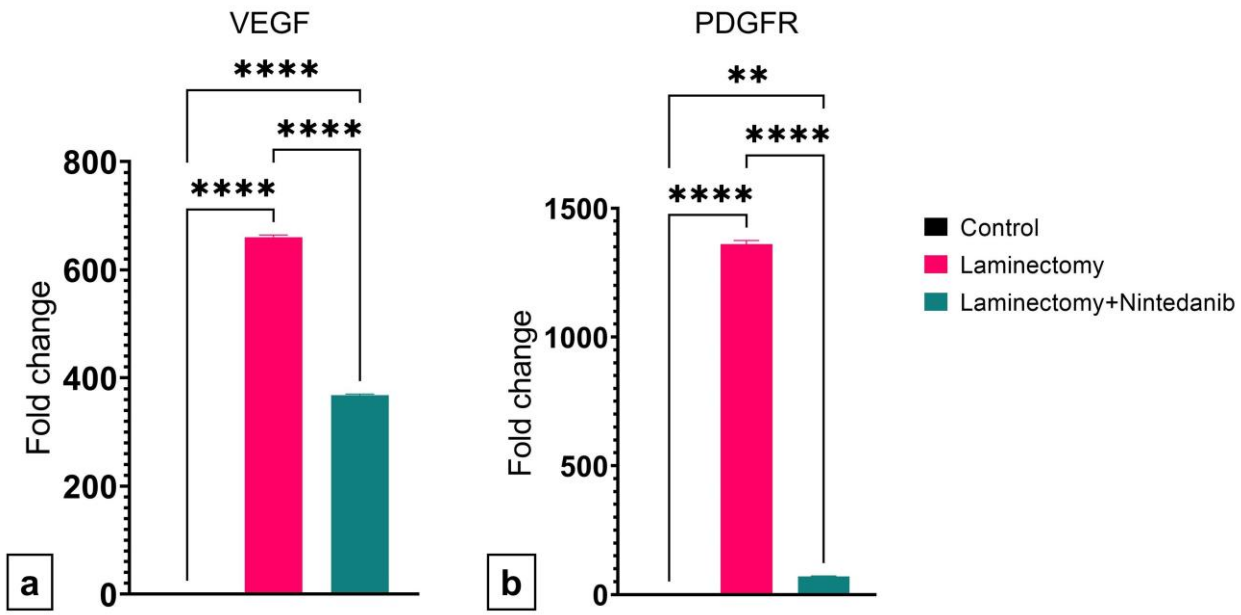


Fig. 5. Quantitative analysis of angiogenic markers by RT-qPCR. (a) VEGF mRNA expression. (b) PDGFR mRNA expression. Data are presented as mean ± SE. Statistical analysis: One-way ANOVA with Tukey's post hoc test (**p < 0.01, ****p < 0.0001).

Accepted artic

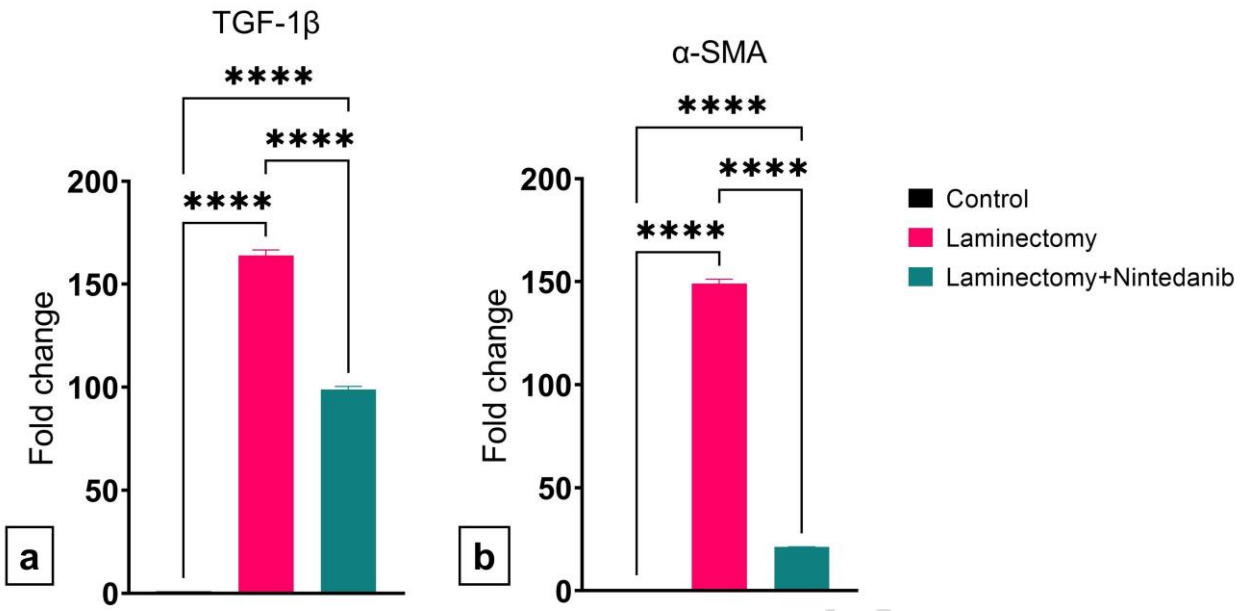


Fig. 6. Quantitative analysis of fibrogenic markers by RT-qPCR. (a) TGF-β1 mRNA expression. (b) α-SMA mRNA expression. Data are presented as mean ± SE. Statistical analysis: One-way ANOVA with Tukey's post hoc test (****$p < 0.0001$).

Accepted artic

Table 1. Primer sequences used for RT-qPCR analysis

Gene	Species	Primer Direction	Sequence (5'-3')	Amplicon Size (bp)
α-SMA	Rat	Forward	5'-AGCCAGTCGCCATCAGGAAC-3'	90 bp
		Revers	5'-CCGGAGCCATTGTCACACAC-3'	
IL-1β	Rat	Forward	5'-GGGCCTCAAGGGGAAGAATC-3'	246 bp
		Revers	5'-ATGTCCCGACCATTGCTGTT-3'	
TNF-α	Rat	Forward	5'-TACTCCCAGGTTCTCTTCAAGG-3'	103 bp
		Revers	5'-GGAGGCTGACTTTCTCCTGGTA-3'	
PDGFR	Rat	Forward	5'-GCACCGAAACAAACACACCTT-3'	144bp
		Revers	5'-ATGTAACCACCGTCGCTCTC-3'	
VEGF	Rat	Forward	5′-TATCTTCAAGCCGTCCTGTG-3′	144 bp
		Revers	5′-TCTCCTATGTGCTGGCTTTG-3′	
TGF-1β	Rat	Forward	5'-TGGCGTTACCTTGGTAACC-3'	277bp
		Revers	5'-GGTGTTGAGCCCTTTCCAG-3'	
GAPDH	Rat	Forward	5'-ATGACTCTACCCACGGCAAG-3'	136bp
		Revers	5'-TACTCAGCACCAGCATCACC-3'	

Primer pairs used to quantify gene expression levels of fibrogenic (α-SMA, TGF-β1), inflammatory (TNF-α, IL-1β), and angiogenic (VEGF, PDGFR) markers in rat spinal tissue. Forward and reverse primer sequences, along with corresponding amplicon sizes (in base pairs), are listed for each target gene. GAPDH was used as the internal reference gene.

Accepted article